Polylactide Nanoparticles Containing Stably Incorporated Cyanine Dyes for In Vitro and In Vivo Imaging Applications

RONG TONG,[1] VIRGINIA J. COYLE,[2] LI TANG,[1] ANNE M. BARGER,[3] TIMOTHY M. FAN,[2*] AND JIANJUN CHENG[1*]
[1]*Department of Materials Science and Engineering, University of Illinois at Urbana-Champaign, Urbana, Illinois 61801*
[2]*Department of Veterinary Clinical Medicine, University of Illinois at Urbana-Champaign, Urbana, Illinois 61801*
[3]*Veterinary Diagnostic Laboratory and Department of Pathobiology, University of Illinois at Urbana-Champaign, Urbana, Illinois 61801*

KEY WORDS polymeric nanoparticles; drug delivery; cancer therapy; chemotherapeutics; cancer targeting; fluorescence imaging; nanomedicine; conjugation; Cy5; PSMA

ABSTRACT Stably incorporating fluorescent molecules to polymeric nanoparticles (NPs) or micelles can facilitate the prolonged tracking of these drug-delivery vehicles in vitro and in vivo. However, incorporation of fluorescent molecules, usually charged and thereby water-soluble, through the encapsulation strategy to hydrophobic polymer matrices is challenging. The encapsulated fluorescent agents are also subject to rapid release when the polymeric NPs are exposed to biological media. To address this issue, we developed Cy5-conjugated polylactide (Cy5-PLA) NPs through Cy5/(BDI)ZnN(TMS)$_2$ [(BDI) = 2-((2,6-diisopropylphenyl)amido)-4-((2,6-diisopropylphenyl)-imino)-2-pentene]-mediated ring-opening polymerization of lactide (LA) followed by nanoprecipitation. This process allows for covalent conjugation of Cy5 to PLA with quantitative incorporation efficiency and formulation of Cy5-PLA NPs with controlled particles size (≈100 nm). As much as 80% of Cy5 was still present in the Cy5-PLA NPs after theses NPs were incubated in PBS at 37°C for 12 days. Cy5-PLA NPs were conjugated to the A10 RNA aptamer that binds to the prostate-specific membrane antigen (PSMA). The resulting Cy5-PLA/aptamer NPs were found to only bind to and get internalized by LNCaP and canine prostate adenocarcinoma cells (PSMA-positive), but not to PC3 cells (PSMA-negative). The Cy5-PLA NPs were administered to balb/c mice intravenously and found to have excellent signals with low-background fluorescence in various organs. *Microsc. Res. Tech. 73:901–909, 2010.*

INTRODUCTION

Polylactide (PLA) represents a class of bioabsorbable and biocompatible polymers that have been extensively used in various biomedical applications such as drug delivery, tissue engineering, in vivo suturing, and coating of medical devices (Caillol et al., 2003; Gottschalk and Frey, 2006; Hagan et al., 1996; Hu et al., 2003; Jing and Hillmyer, 2008; Kumar et al., 2002; Stolnik et al., 2001). When used for drug-delivery vehicle preparations, PLA usually constitutes the hydrophobic segments of amphiphilic copolymers for the assembly of polymeric micelles (Arimura et al., 2005; Avgoustakis, 2004; Hagan et al., 1996; Hu et al., 2003; Iijima et al., 1999; Ishihara et al., 2009; Jiang et al., 2009; Lee et al., 2007; Liu et al., 2001; Nagasaki et al., 1998; Nederberg et al., 2009; Otsuka et al., 2000; Pierri and Avgoustakis, 2005; Stolnik et al., 1994; Wu et al., 2005; Yang et al., 2009; Zhang and Feng, 2006a,b; Zhang et al., 1996) or can be directly adopted for preparing polymeric nanoparticles (NPs) to encapsulate therapeutic agents (Figs. 1A and 1B) (Alexis et al., 2008; Peer et al., 2007; Zhang et al., 2008). These formulation methods are typically used for the incorporation of hydrophobic agents that are embedded in PLA matrices (Esmaeili et al., 2008; Nederberg et al., 2009). The efficiency for loading water-soluble drugs or dyes to PLA micelles or NPs is generally very low. In addition, the encapsulated functional agents are typically released from PLA micelles and NPs rapidly via so-called burst-release mechanism (Huang and Brazel, 2001) with over 60–90% of the agents being released within the first few or tens of hours (Musumeci et al., 2006; Soppimath et al., 2001). To monitor the in vitro and in vivo performance of PLA-based drug-delivery vehicles, it would be ideal to develop in parallel-imaging agents, which can be incorporated with sufficient stability in PLA matrices.

Many commercially available fluorescent dyes are charged molecules and therefore have excellent water solubility. During micellation or nanoprecipitation, a large portion of these dye molecules tends to stay in aqueous phase instead of being encapsulated and embedded in PLA. Even for the small amount of dyes being encapsulated, they are still subject to rapid

R.T. and V.J.C. contributed equally to this work.

*Correspondence to: Jianjun Cheng, Department of Materials Science and Engineering, University of Illinois at Urbana-Champaign, 1304 West Green Street, Urbana, Illinois 61801, USA. E-mail: jianjunc@illinois.edu; Timothy M. Fan, Department of Veterinary Clinical Medicine, University of Illinois at Urbana-Champaign, Urbana, Illinois 6180, USA. E-mail: t-fan@illinois.edu

Received 8 December 2009; accepted in revised form 21 December 2009

Contract grant sponsor: National Science Foundation (Career Award Program); Contract grant number: DMR-0748834; Contract grant sponsor: National Institutes of Health; Contract grant numbers: 1R21CA139329, 1R21EB009486-01; Contract grant sponsor: Siteman Center for Cancer Nanotechnology Excellence (SCCNE, Washington University)—Center for Nanoscale Science and Technology (CNST, University of Illinois at Urbana—Champaign)

DOI 10.1002/jemt.20824

Published online 9 February 2010 in Wiley Online Library (wileyonlinelibrary.com).

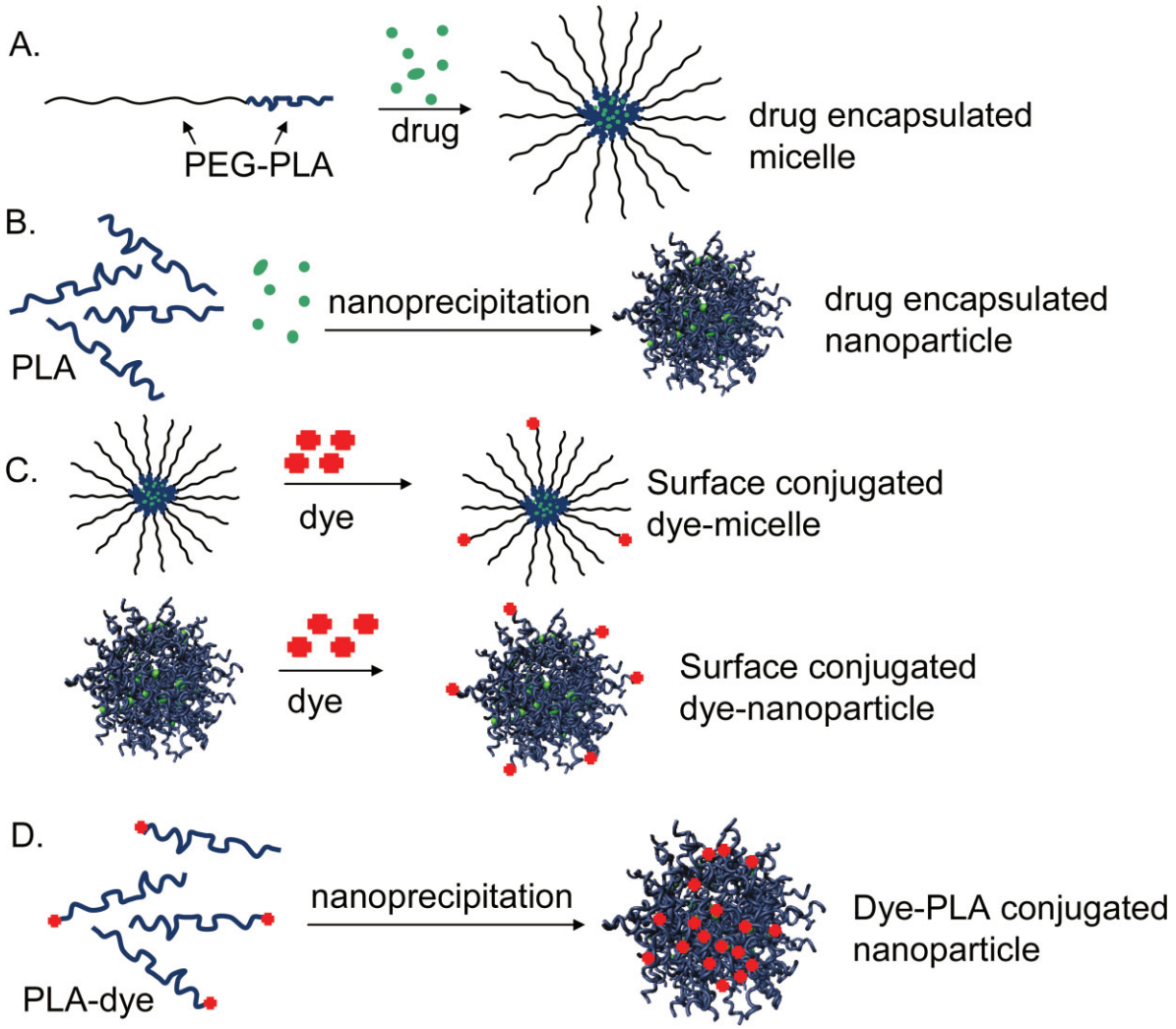

Fig. 1. Schematically illustration of the formation of (**A**) amphiphilic mPEG-PLA micelles and (**B**) nanoparticles via nanoprecipitation. **C:** Illustration of conjugating dyes to the external surface of nanoparticles or micelles. **D:** Illustration of conjugating dyes to PLA followed by nanoprecipitation to form dye-stably incorporated nanoparticles. [Color figure can be viewed in the online issue, which is available at wileyonlinelibrary.com.]

release via "burst-release" mechanism. One method to solve this problem is to conjugate lipophilic motifs with long alkyl chains to the water-soluble fluorescence molecules (e.g., DiIC18 by Invitrogen) to assemble with the hydrophobic domains in nanodevices. To stably incorporate water-soluble dyes within polymeric NPs or micelles and thereby allowing for prolonged tracking of these nanodevices in vitro or in vivo using fluorescence techniques, an alternative strategy is to covalently conjugate fluorescent molecules to the surface of the preformed nanodevices (Fig. 1C). However, both strategies may be subject to rapid cleavage in vivo induced by reduced pH (e.g., in tumor tissue, in gastrointestinal tract, or in subcellular organelles) (Cheng et al., 2004, 2006a,b; Chi and Pizzo, 2006; Lee et al., 2005; Murdter et al., 2002; Teply et al., 2008; Verma et al., 2008) or by digestive enzymes, and/or uncontrolled release from these nanodevices when they are directly exposed to harsh in vitro or in vivo environments. The cellular trafficking and in vivo biodistribution properties of these surface-modified nanodevices may also be altered, especially with high density of fluorescent dyes. We envisioned that covalently conjugating fluorescent agents directly to PLA and subsequently using the PLA-dye conjugates for the formation of micelles or NPs should avoid all these issues mentioned earlier to a large extent. The dye molecules attached to hydrophobic PLA domains should be homogeneously distributed within PLA matrices. During micellation or nanoprecipitation, a large portion of dye molecules are hence localized inside NPs or micelles with minimum contact with the external environment (Fig. 1D). Covalent conjugation of dyes to PLA will also greatly reduce drug release and avoid the burst release issues. The substantially improved stability of dyes in PLA-based NPs or micelles will facilitate the prolonged tracking of these delivery devices in vitro and in vivo via conventional fluorescent methodologies.

PLAs are usually prepared via the ring-opening polymerization of lactide (LA) initiated by a hydroxyl-con-

taining agent (Kumar et al., 2002). This strategy has been routinely used for incorporating small molecules or polymers to the termini of PLAs. The ring opening polymerization of LA mediated by Sn(II) 2-ethylhexanoate is particularly attractive, because the catalyst is easily accessible and has low toxicity (Dechy-Cabaret et al., 2004; Gerhardt et al., 2006). However, this reaction requires high temperature (120°C or higher), which may not be suitable for temperature-sensitive agents. The resulting PLAs also usually have poorly controlled molecular weights (MWs) and broad molecular weights distribution (MWDs). Recently, we developed a method that allowed incorporation of hydroxyl-containing chemotherapeutics agents under mild condition, which allowed for the preparation of PLA-drug conjugates with controlled MWs and narrow MWDs (Tong and Cheng, 2008, 2009, 2010; Tong et al., 2009c). Here, we report the use of this method for the formulation PLA NPs containing covalently conjugated Cy5, a hydrophilic, near infrared fluorescent dye with excitation wavelength of 649 nm and emission wavelength of 670 nm. We demonstrated that Cy5-PLA NPs can be easily prepared with controlled particle size and narrow size distribution with 100% of Cy5 incorporation efficiency. To demonstrate the biologically relevant applications of these NPs, we modified the surface of Cy5-PLA NPs with A10 aptamer, an oligonucleotide ligand that targets prostate-specific membrane antigen (PSMA), a transmembrane protein expressed by prostate carcinoma, and tumor-associated neovasculature (Lupold et al., 2002). We demonstrated that these Cy5-PLA/aptamer NPs are highly selective for the binding and imaging of PSMA-expressing prostate cancer cells in vitro. Additionally, we also performed preliminary in vivo studies demonstrating that Cy5-PLA NPs can be easily visualized in various visceral organs with low-autofluorescent background ratios. These promising results support the further development of Cy5-PLA NPs as an excellent model system to assess the in vitro and in vivo pharmacological and pharmacokinetical profiles of polymeric nanomedicine.

MATERIALS AND METHODS

General

D,L-LA was purchased from TCI America (Portland, OR), recrystallized three times in toluene, and stored at −30°C in a glove box prior to use. The beta-diimine (BDI) ligand [(BDI) = 2-((2,6-diisopropylphenyl)amido)-4-((2,6-diisopropylphenyl)-imino)-2-pentene] and the corresponding metal catalysts ((BDI)ZnN(TMS)$_2$) were prepared by following the published procedures (Chamberlain et al., 2001) and stored at −30°C in a glove box before use. All anhydrous solvents were purified by passing them through dry alumina columns and kept anhydrous using molecular sieves in a glove box. Cy5 was synthesized according to the previously reported procedure (Southwick et al., 1990). All other chemicals were purchased from Sigma-Aldrich (St Louis, MO) and used as received unless otherwise specified. The MWs of the Cy5-PLA were determined on a gel permeation chromatograph (GPC, also called size-exclusion chromatography) equipped with an isocratic pump (Model 1100, Agilent Technology, Santa Clara, CA), a DAWN HELEOS 18-angle laser light scattering detector (Wyatt Technology, Santa Barbara, CA), and an Optilab rEX refractive index detector (Wyatt Technology). The wavelength of the HELEOS detector was set at 658 nm. The size exclusion columns (Phenogel columns 100 Å, 500 Å, 10^3 Å, and 10^4 Å, 5 μm, 300 × 7.8 mm, Phenomenex, Torrance, CA) used for the analysis of polymers or polymer-drug conjugates were serially connected on the GPC. The GPC columns were eluted with THF (HPLC grade) at 40°C at 1 mL/min. HPLC analyses were performed on a System Gold system (Beckman Coulter, Fullerton, CA) equipped with a 126P solvent module, a System Gold 128 UV detector, and an analytical pentafluorophenyl column (Curosil-PFP, 250 × 4.6 mm, 5 μ, Phenomenex, Torrance, CA) or an analytical C18 column (Luna C18, 250 × 4.6 mm, 5 μ, Phenomenex, Torrance, CA). The UV wavelength for detecting Cy5 was set at 550 nm. The NMR experiments were conducted on a Varian U500, a VXR500, or a UI500NB (500 MHz) NMR spectrometer. The size and particle dispersity of the PLA-Cy5 NPs were measured on a Zeta-Plus dynamic light scattering (DLS) detector (15 mW laser, incident beam = 676 nm, Brookhaven Instruments, Holtsville, NY). The TEM analysis was performed on a JEOL 2100 Cryo-TEM system.

Synthesis of Cy5-PLA Conjugates

In a glove box, Cy5 (2.5 mg, 0.005 mmol) was dissolved in anhydrous THF (1 mL). (BDI)ZnN(TMS)$_2$ (7.0 mg, 0.01 mmol) in THF (100 μL) was added to the Cy5 solution. The mixture was stirred for 15–20 min at room temperature. LA (72 mg, 0.5 mmol) in anhydrous THF (2 mL) was added dropwise to the vigorously stirred mixture of Cy5 and (BDI)ZnN(TMS)$_2$. The polymerization was monitored by following the lactone band at 1772 cm^{-1} using FTIR or by checking the methine (—C*H*—) peak of LA using ^{1}H NMR. After the polymerization was complete, an aliquot of the polymerization solution was measured by HPLC to quantify the unreacted Cy5 to determine the incorporation efficiency of Cy5 to the Cy5-PLA conjugate. The resulting Cy5-PLA was precipitated with methanol/acetic acid (vol/vol = 100/1, 10 mL) to remove the BDI ligand and then dried under vacuum. Complete removal of BDI was confirmed by NMR, HPLC, and thin-layer chromatography. After the organic solvent was evaporated, the residue was dissolved in THF (10 mg/mL, HPLC grade) and analyzed by GPC.

Preparation of Cy5-PLA-Conjugated NPs

The Cy5-PLA-conjugated NPs were readily prepared through the nanoprecipitation of Cy5-PLA conjugates in the presence of PLA-monomethoxy poly(ethylene glycol) (PLA-mPEG) (Fig. 2). Briefly, Cy5-PLA conjugate (100 μL DMF, 10 mg/mL) and PLA-mPEG (100 μL DMF, 10 mg/mL) were mixed and then added dropwise to nanopure water (4 mL). The resulting NP suspension was purified by ultrafiltration (15 min, 3000 rpm, Ultracel membrane with 10,000 NMWL, Millipore, Billerica, MA) and then characterized by DLS and TEM.

Preparation of Cy5-PLA/Aptamer-Conjugated NPs

Cy5-PLA/PLA-PEG-COOH NPs (w/w = 1/1, 1 mL, 1 mg/mL in DNase RNase-free water) were incubated in aqueous solution containing 1-(3-dimethylaminopropyl)

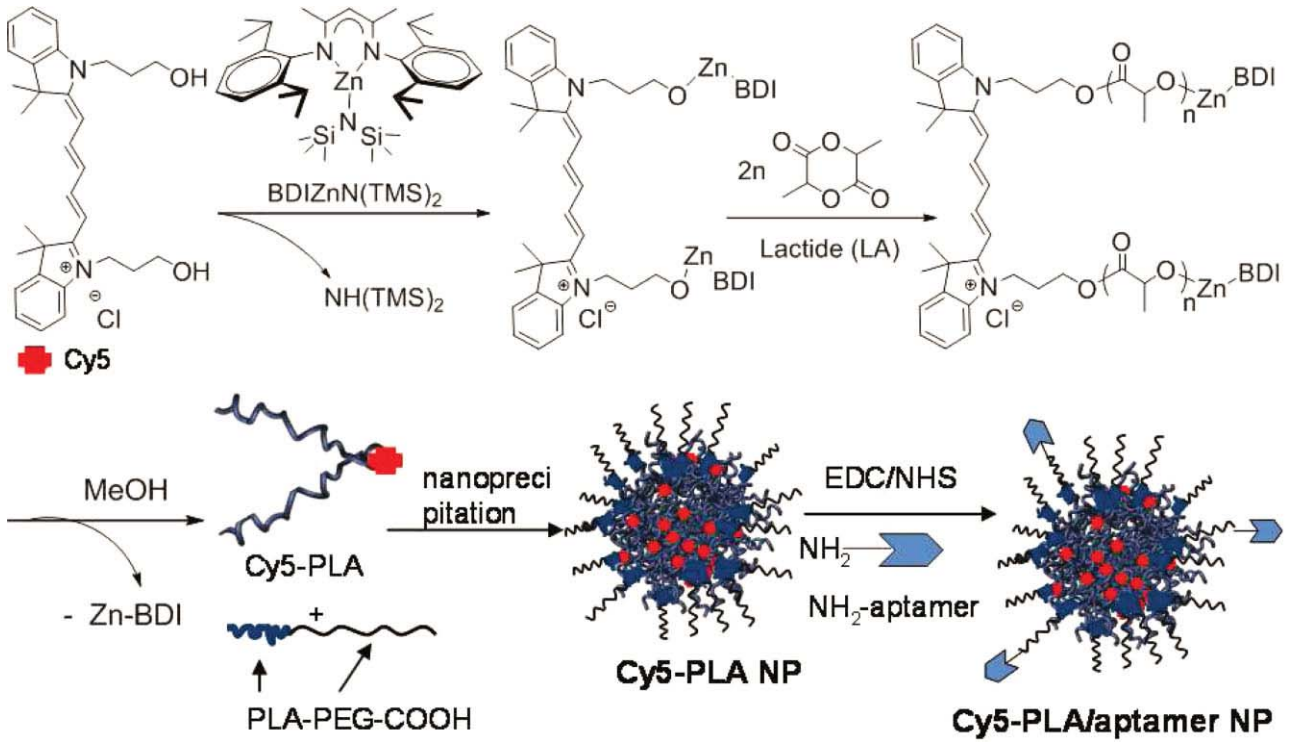

Fig. 2. Preparation of Cy5-PLA/aptmaer nanoparticles via Cy5 initiated LA polymerization in the presence of (BDI)ZnN(TMS)2 followed by conanoprecipitation with polylactide-*b*-methoxylated PEG (PLA-mPEG5K) and conjugation with amine-terminated A10 aptamer. [Color figure can be viewed in the online issue, which is available at wileyonlinelibrary.com.]

-3-ethylcarbodimide (EDC) hydrochloride (400 mM, 200 μL) and *N*-hydroxysuccinimide (NHS) (100 mM, 200 μL) for 15 min at room temperature. The resulting NHS-activated NPs were allowed to react with 5′-NH_2-modified A10 PSMA aptamer (1 μg/μL in DNase RNase-free water, 50 μL). The resulting NP-aptamer bioconjugates were washed with ultrapure water (15 mL) by ultrafiltration (5 min, 1000*g*, Ultracel membrane with 10,000 NMWL, Millipore, Billerica, MA). The aptamer-modified NPs were resuspended (1 mg/mL in DNase RNase-free water) and analyzed by fluorescence-activated cell sorting (FACS, BD FACScan™ Flow Cytometer) and fluorescence microscopy (Leica SP2 Laser Scanning Confocal Microscope).

Cell Culture

The canine prostate adenocarcinoma line (CPA) was provided by Monique Dore, (University of Montreal). The LNCaP and PC3, two human prostate carcinoma lines, were purchased from American Tissue Culture Collection. The human LNCaP and PC3 cell lines served as positive and negative controls for PSMA gene expression, respectively. Both CPA and LNCaP cell lines were cultured in RPMI 1640 (Gibco, Grand Island, NY) supplemented with 2 mM L-glutamine (Gibco, Grand Island, NY) and 10% fetal bovine serum. The PC3 cell line was grown in complete F12 media (Gibco).

PSMA mRNA Assessment of Cells

Total RNA was collected from LNCaP, PC3, and CPA cells with a commercially available kit (Qiagen) and 1 μg of total RNA was reverse-transcribed to cDNA. Five microliters of reverse transcribed product were used as a template in a 50-μL polymerase chain reaction containing 100 ng of each oligonucleotide, 2.5 U of AmpliTaqGold, and forward (5′-GGA AAT CCC ATC ACC ATC TTC CA-3′) and reverse (5′-CAT CAC GCC ACA GTT TCC CGG AG-3′) degenerate primers for human and canine PSMA. Reactions were performed in a PTC-200 Peltier thermal cycler with the following cycling conditions: 5 min at 94°C denaturing step, followed by 32 cycles (60 s at 94°C, 90 s at 55°C, and 60 s at 72°C) and concluded by 72°C for 10 min.

Immunocytochemistry Using Antibodies for the Confirmation of PSMA Protein Expression

A mouse monoclonal antihuman PSMA antibody, clone Y-PSMA-1 (Abcam, Cambridge, MA), was used to confirm PSMA protein expression in human and canine cell lines. The secondary antibody used was a goat anti-mouse HRP-conjugated antibody (DAKO Corporation, Carpinteria, CA). Cytospin preparations of all cell lines (LNCaP, PC3, and CPA) were incubated in acetone for 10 min, allowed to air dry, and loaded on the DAKO autostainer (DAKO Corporation). To minimize nonspecific peroxidase background staining, all preparations were blocked with 10% hydrogen peroxide for 20 min. Cytospin preparations were incubated with mouse monoclonal antihuman PSMA antibody at a 1:100 dilution for 30 min. Subsequently, samples were incubated with secondary goat anti-mouse immunoglobulin for 30 min, followed by 3,3′-diaminobenzidine

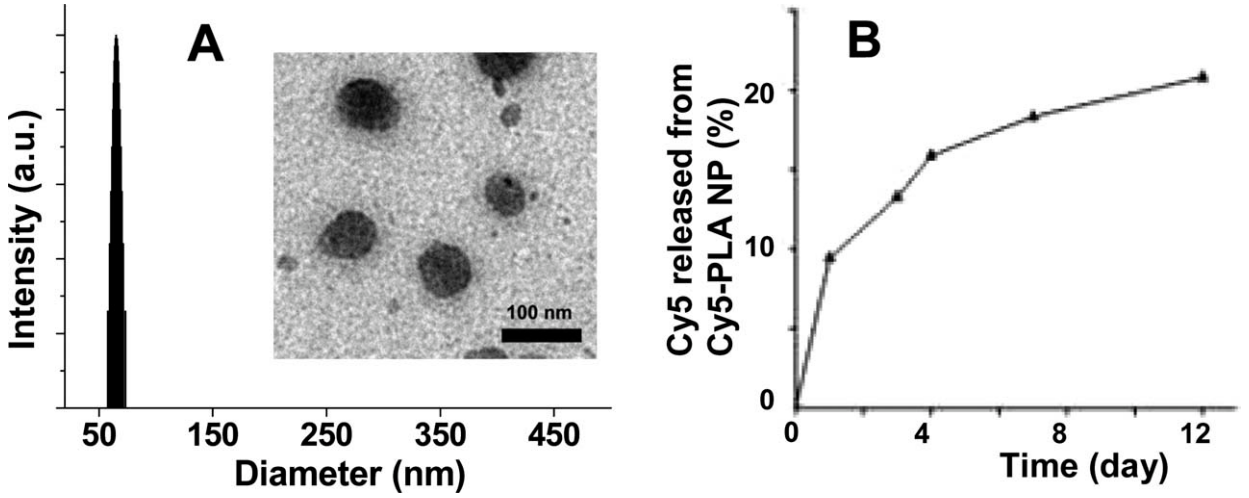

Fig. 3. Characterization of Cy5-PLA/PLA-PEG-mPEG nanoparticles by dynamic light scattering (DLS) (**A**) and transmission electron microscopy (TEM) (Inset). **B:** Release kinetics Cy5 from Cy5-PLA NP in PBS at 37°C.

chromagen solution for 7 min, and then counterstained with Mayer's hematoxylin for 5 min (DAKO Corporation). The LNCaP and PC3 cell lines were used as PSMA positive and negative control, respectively. Positive PSMA protein expression was characterized by membranous staining with or without cytoplasmic staining.

Confocal Microscopy for In Vitro Imaging of PSMA-Targeted Cy5-PLA/Aptamer NPs

The LNCaP, PC3, and CPA cells were plated in chamber slides in corresponding media for 24 h. Cells were then washed with PBS and incubated for an additional 6 h with either 100 μL of Cy5-PLA aptamer NP (treatment group) or Cy5-PLA NP (control group). Cells were then washed with PBS thrice to remove all unbound NPs and fixed with 4% paraformaldehyde for 5 min. Cells were rinsed with PBS, incubated with Alexa-Fluor Phalloidin to counter stain F-actin fibers within the cytoskeleton, and then analyzed by confocal fluorescent microscopy.

In Vivo Evaluation of Cy5-PLA NP Biodistribution

Three female balb/c mice were injected each with Cy5-PLA NP (1 mg, 300 μL PBS) via lateral tail vein and then sacrificed 24 h later. One untreated balb/c mouse was sacrificed and used as an autofluorescence background control. The in vivo biodistribution of Cy5-PLA NP within visceral organs including heart, lung, liver, spleen, and kidney was studied using a LI-COR Odyssey scanner (LI-COR Bioscience, Lincoln, NE).

RESULTS AND DISCUSSION

Synthesis and Characterization of Cy5-PLA Nanoconjugates

We have previously reported that hydroxyl-containing therapeutic molecules, such as paclitaxel (Tong and Cheng, 2008) and doxorubicin (Tong and Cheng, 2009), could function as initiators for controlled polymerization of LA when the polymerizations were mediated by $(BDI)ZnN(TMS)_2$ (Chamberlain et al., 2001). Paclitaxel-PLA and doxorubicin-PLA conjugates were prepared with controlled MWs and narrow MWDs. Because Cy5 has two hydroxyl groups, we anticipated that Cy5-PLA conjugates could be similarly prepared using this method. Cy5 is thus stably incorporated to PLA, as releasing each Cy5 molecule from Cy5-PLA conjugates requires the cleavage of two ester bonds (Fig. 2).

We prepared Cy5-PLA conjugates via Cy5/$(BDI)ZnN(TMS)_2$-mediated LA polymerization at a LA/Cy5 ratio of 100. The obtained M_n of Cy5-PLA was 1.27×10^4 g/mol, which was in good agreement with the expected MW (1.52×10^4 g/mol). The Cy5-PLA also had a very narrow MWD ($M_w/M_n = 1.03$), which is consistent with what we reported previously for paclitaxel(doxorubicin)/$(BDI)ZnN(TMS)_2$ mediated controlled polymerization of LA (Tong and Cheng, 2008, 2009). Cy5-PLA conjugates prepared at a LA/Cy5 ratio of 200 and 300 were also synthesized using the same method, both of which have the expected M_n's and very narrow MWDs (data not shown). Because the syntheses of Cy5-PLA conjugates are straightforward, gram-scale Cy5-PLA conjugates with well-controlled compositions and MWs can be easily prepared using this dye-initiated polymerization method and used for the preparation of Cy5-PLA NPs.

Nanoprecipitation has been extensively used for the rapid preparation of NPs with therapeutic agents embedded in the hydrophobic polymeric matrices. Generally, a mixture of hydrophobic polymer and drug is dissolved in water-miscible organic solvent (e.g., DMF or acetone) and then added dropwise to a vigorously stirred water solution ($V_{water}/V_{solvent} = 10–40$). The instantaneous diffusion of the organic solvent into water results in the formation of polymeric NPs with drugs embedded. The nanoprecipitation of Cy5-PLA resulted in Cy5-PLA NPs with size 64.5 ± 0.9 nm by DLS. These Cy5-PLA NPs have monomodal particle size distributions and low polydispersities (Fig. 3A). The narrow, monomodal particle size distribution for NPs

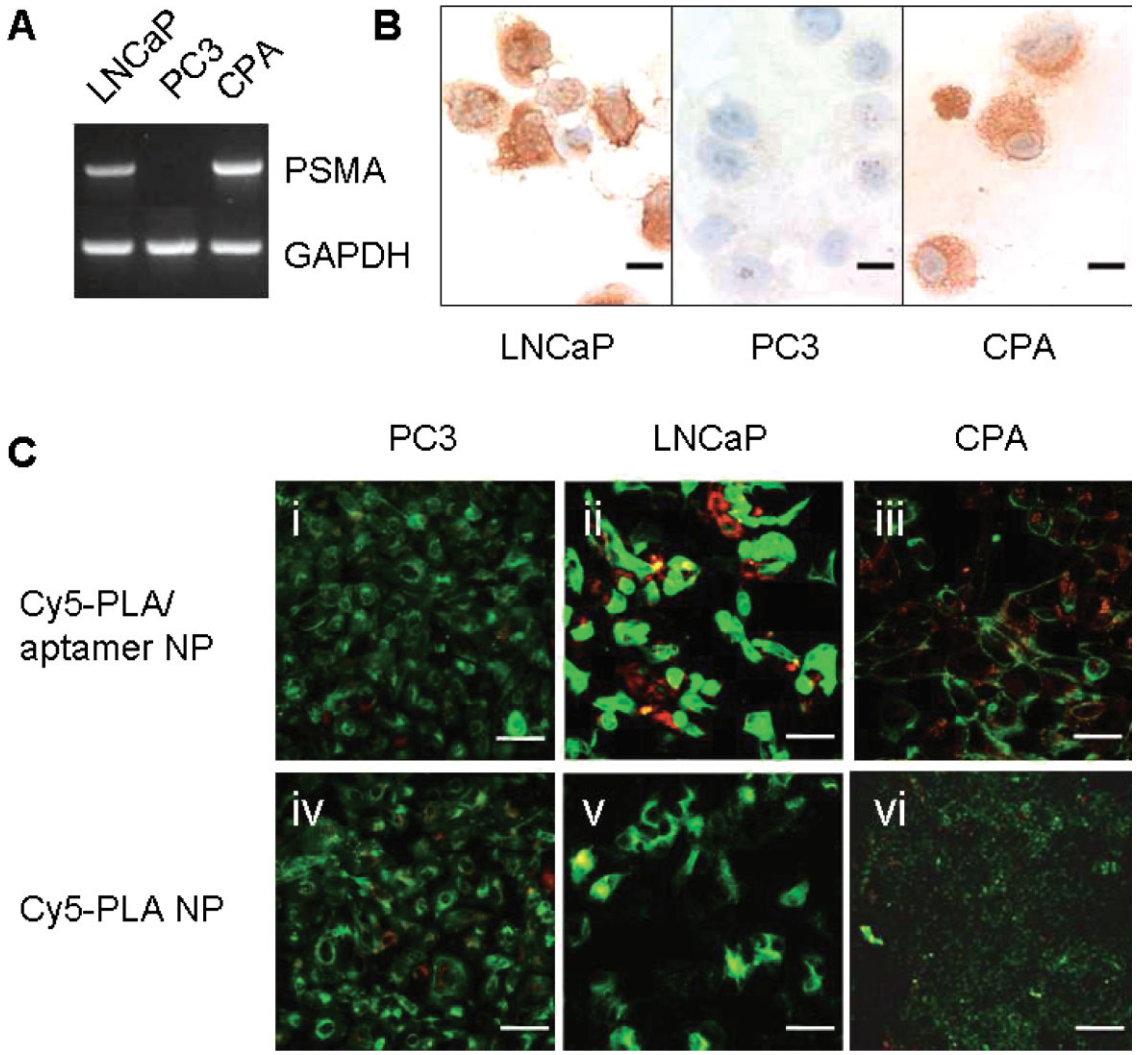

Fig. 4. In vitro evaluation of Cy5-PLA NPs with or without surface-conjugated PSMA-aptamer for cancer targeting. **A:** Qualitative polymerase chain reaction confirming messenger RNA transcription of the PSMA gene in CPA and LNCaP, but not in PC3, prostate carcinoma cell lines. **B:** Translation of PSMA protein demonstrated in cytospin preparations of CPA and LNCaP, but not PC3, prostate carcinoma cell lines; positive PSMA staining indicated by diffuse membranous staining pattern (500× magnification); Bar = 20 μm. **C:** Binding and internalization of Cy5-PLA NPs with or without surface-conjugated PSMA-aptamer in PC3 (PSMA−), LNCaP (PSMA+), and CPA (PSMA+) cells: (**i** and **iv**, PC3 cells treated with Cy5-PLA NP and Cy5-PLA/aptamer NP, respectively), (**ii** and **v**, LNCaP cells treated with Cy5-PLA NP and Cy5-PLA/aptamer NP, respectively), (**iii** and **vi**, CPA cells treated with Cy5-PLA NP and Cy5-PLA/aptamer NP, respectively); Bar = 50 μm. [Color figure can be viewed in the online issue, which is available at wileyonlinelibrary.com.]

derived from the Cy5-PLA conjugates was confirmed by TEM (inset, Fig. 3A), which is in sharp contrast to the multimodal particle size distribution typically observed with the NPs prepared by the coprecipitation of a mixture of small molecule agents and hydrophobic polymers (Cheng et al., 2007; Farokhzad et al., 2006). The multimodal size distribution of NPs prepared by coprecipitation is due in part to the aggregation of the nonencapsulated drug molecules. However, using Cy5-initiated LA controlled polymerization followed by nanoprecipitation, Cy5-PLA NPs with monomodal particle size distribution and very low polydispersities are easily attainable, which is likely related to the unimolecular structures of the Cy5-PLA conjugates.

Slow release of Cy5 from Cy5-PLA NP was observed through the hydrolysis of the ester linker connecting the Cy5 and the PLA (Fig. 3B) with no "burst release" of Cy5 being observed. As much as 80% of Cy5 is still stably conjugated to PLA NP, after the Cy5-PLA, NPs were incubated in PBS at 37°C for 12 days (Fig. 3B). This observation was in sharp contrast to the burst release of PLA/Cy5 NP prepared by coprecipitation, in which Cy5 release depends entirely on diffusion with over 90% of embedded Cy5 being released within 24 h (data not shown).

Conjugation of PSMA-Aptamer to Cy5-PLA NPs

Aptamers are single-stranded DNAs or RNAs that can specifically bind to target ligands, such as cell-surface markers or other transmembrane proteins.

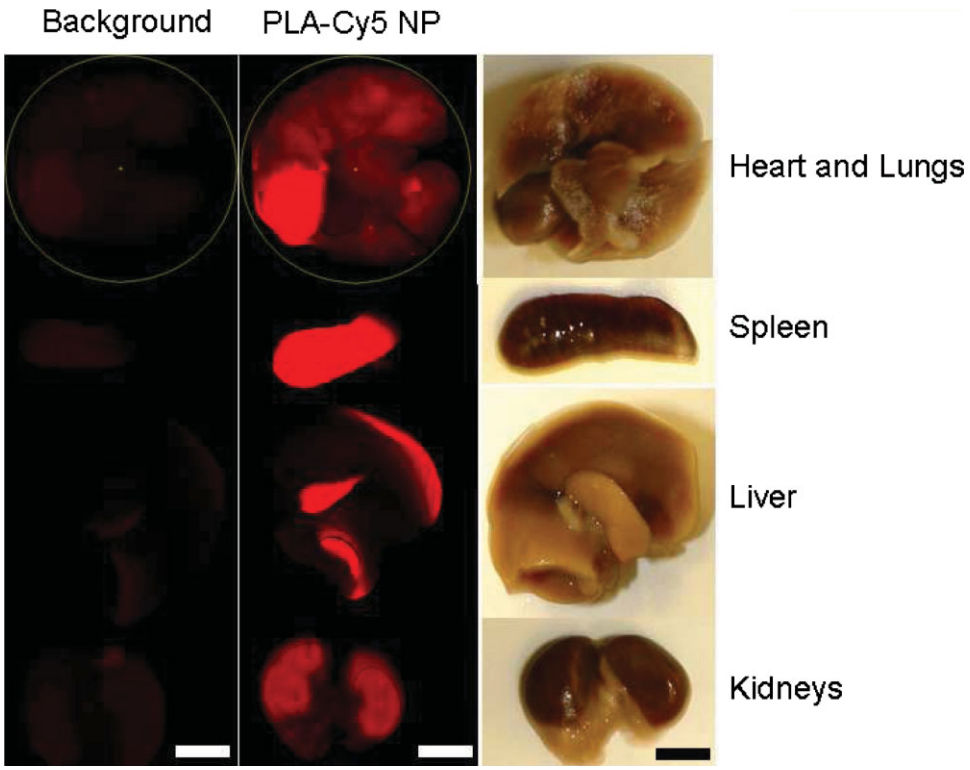

Fig. 5. In vivo biodistribution of intravenously administered Cy5-PLA NP. Visceral organ biodistribution of Cy5-PLA NP following lateral tail vein injection using the LI-COR Odyssey scanner. Accumulation of Cy5-PLA NP within visceral organs allows for greater than >10-fold increase in fluorescent intensity in comparison with background autofluorescence. Splenic accumulation of Cy5-PLA NP is the greatest for all visceral organs examined (spleen, liver, kidney, lung, and heart); Bar = 5 mm. [Color figure can be viewed in the online issue, which is available at wileyonlinelibrary.com.]

Aptamers are generally selected from a library of nucleic acids with random sequences via a combinatorial process called systematic evolution of ligands by exponential enrichment (SELEX) (Ellington et al., 1990, 1992; Tuerk and Gold, 1990). When used for cancer targeting, aptamers are able to bind to target antigens with extremely high affinity and specificity in a manner resembling antibody-mediated cancer targeting. An A10 aptamer with 2′-fluoro-modified ribose on all pyrimidines and a 3′-inverted deoxythymidine cap has been identified via SELEX and used to target the extracellular domain of PSMA (Lupold et al., 2002). The A10 aptamer binds to the PSMA-positive LNCaP prostate cancer cells but not PSMA-negative PC3 prostate cancer cells. Previous studies showed that PLGA-PEG-aptamer bioconjugates were able to target LNCaP cells in vitro and in vivo (Bagalkot et al., 2006; Farokhzad et al., 2004, 2006).

In our investigation, A10 aptamers were conjugated onto Cy5-PLA NPs to determine their suitability for studying cancer cell targeting in vitro. The amine-terminated A10 aptamer was conjugated to the PLA-PEG-COOH/Cy5-PLA NPs, with particle size of 132.8 nm and polydispersity of 0.031, through the carboxylic acid-amine coupling reaction in the presence of EDC and NHS to give aptamer-coated PLA-PEG-COOH/Cy5-PLA NPs (Cy5-PLA/aptamer NP) (Farokhzad et al., 2004). After purifying the Cy5-PLA/aptamer NPs by centrifugation and washing the NPs with PBS, we found that the size of Cy5-PLA/aptamer NPs increased slightly to 157.1 nm with a polydispersity of 0.144.

In Vitro Imaging Study of Aptamer-Cy5 NPs for Prostate Cancer Targeting

Before testing the selectivity of our Cy5-PLA/aptamer NPs for the recognition of PSMA, we performed a series of in vitro assays to confirm the expression of PSMA in the LNCaP, a known PSMA expressing cell line, and an additional cell line called CPA, a canine prostate cancer cell. We chose to study CPA in our investigation, because naturally occurring prostate carcinoma in dogs may serve as an excellent comparative model for prostate cancer in men (LeRoy and Northrup, 2009). Furthermore, the expression of PSMA in the majority of spontaneously arising canine prostate carcinomas appears to be a shared similarity between humans and canines (Lai et al., 2008; Sweat et al., 1998). As expected, messenger RNA for PSMA was detected in CPA, which was identical to that of human prostate carcinoma cell lines (LNCaP) that served as positive control (Fig. 4A). Also as expected based upon PSMA promoter hypermethylation, no amplicons were detectable for the human PC3 prostate carcinoma cell line that was used a negative control in this study (Fig. 4A). Messenger RNA transcripts were effectively translated into membranous-bound protein in CPA as demonstrated by positive immunocytochemi-

cal staining with LNCaP and PC3 being used the positive and the negative control, respectively (Fig. 4B). These studies confirmed that PSMA is expressed in both LNCaP and CPA cells.

We then explored the selective targeting capability of Cy5-PLA NPs and Cy5-PLA/aptamer NPs to PSMA-positive LNCaP and CPA cells as well as PSMA-negative PC3 cells. Because PC3 cells do not express the PSMA protein, there was essentially no difference between the Cy5-PLA/aptamer NP and the Cy5-PLA NP without aptamer with respect to their capability of cell-binding and internalization (i and iv, Fig. 4C). The uptake of Cy5-PLA NPs to both LNCaP and CPA cells was significantly enhanced when NPs were coated with aptamer (ii vs. v for LNCaP, iii vs. vi for CPA, Fig. 4C); membranous protein expression of PSMA by the LNCaP and CPA cell lines allowed for the selective in vitro targeting of this canine cancer cell with Cy5-PLA/aptamer NPs, but not Cy5-PLA NP. These in vitro studies demonstrated that NPs conjugated with aptamer-targeting ligand with stably incorporated Cy5 are excellent substrates to study NP-mediated cancer targeting.

In Vivo Biodistribution of Cy5-PLA Nanoconjugates

There is growing interest for developing fluorescent imaging techniques to monitor the physiological passage of drug-delivery NPs in vivo. To ensure effective measurement of fluorescent signals in vivo, it is crucial to use red or near-IR dyes whose fluorescent intensities have excellent tissue penetration capability, allowing for high-resolution imaging of internal organs. The Cy5-PLA NPs have small sizes (less than 200 nm) and low-size distribution, and contain stably incorporated Cy5. We next tested whether the biodistribution of these NPs could be visualized in various visceral organs with fluorescence techniques after they are systemically injected into mice.

To demonstrate the potential use of Cy5-PLA NPs as a fluorescence imaging agent, we administered Cy5-PLA NP to three female balb/c mice via lateral tail vein injection. Large amounts of Cy5-PLA NP (50 mg/kg, 300 μL) were safely injected into living mice without adverse or acute biological consequences such as immediate or sudden death following intravenous delivery. After the injections, we were able to characterize the biodistribution of Cy5-PLA NPs in balb/c mice through the use of a highly sensitive fluorescent scanner (LI-COR Odyssey scanner). Twenty-four hours following intravenous injection, Cy5-PLA NPs were detected at the highest concentration within the spleen (fluorescent intensity 20-fold greater than background splenic tissue autofluorescence). Additionally, the presence of Cy5-PLA NPs was also readily identified in the liver, heart, kidney, and lungs (Fig. 5). The chemical stability of fabricated Cy5-PLA NP, in conjunction with the high-detail tissue resolution (21 μm) capacity of the LI-COR Odyssey scanner, allows the possibility to study the biodistribution and biologic fate of Cy5-PLA NP following administration to mice. The combined technologies of Cy5-PLA NP and LI-COR Odyssey scanner will be useful for studying the capability of PLA NPs to preferentially localize and penetrate into established tumors in living mice.

CONCLUSION

In conclusion, we developed Cy5-initiated LA polymerization for the preparation of Cy5-PLA conjugates with Cy5 being stably conjugated. The resulting Cy5-PLA conjugates have well-controlled MWs and narrow MWDs, allowing for the formulation of Cy5-PLA NPs with controlled particle size and narrow particle size distribution. Cy5-PLA NPs were effectively used for assessing in vitro targeting when PSMA-aptamer was conjugated to the surface of Cy5-PLA NPs. Cy5-PLA NPs were also systemically administered to mice and found to have excellent signals with low-background fluorescence. This class of fluorescent, polymeric NPs with Cy5-stably incorporated can potentially be excellent substrates for the rapid assessment of NP biodistribution in vivo.

ACKNOWLEDGMENTS

R.T. acknowledges a student fellowship from SCCNE. We thank Professors Martin Burke for helping on anhydrous solvents. We also thank Professor Edward Roy and Diana Thomas for aiding with mice organ image acquisition using the LI-COR Odyssey scanner system.

REFERENCES

Alexis F, Rhee JW, Richie JP, Radovic-Moreno AF, Langer R, Farokhzad OC. 2008. New frontiers in nanotechnology for cancer treatment. Urol Oncol-Semin Orig Invest 26:74–85.

Arimura H, Ohya Y, Ouchi T. 2005. Formation of core-shell type biodegradable polymeric micelles from amphiphilic poly(aspartic acid)-*block*-polylactide diblock copolymer. Biomacromolecules 6:720–725.

Avgoustakis K. 2004. Pegylated poly(lactide) and poly(lactide-*co*-glycolide) nanoparticles: Preparation. Properties and possible application in drug delivery. Curr Drug Deliv 1:321–333.

Bagalkot V, Farokhzad OC, Langer R, Jon S. 2006. An aptamer-doxorubicin physical conjugate as a novel targeted drug-delivery platform. Angew Chem Int Ed 45:8149–8152.

Caillol S, Lecommandoux S, Mingotaud AF, Schappacher M, Soum A, Bryson N, Meyrueix R. 2003. Synthesis and self-assembly properties of peptide—Polylactide block copolymers. Macromolecules 36:1118–1124.

Chamberlain BM, Cheng M, Moore DR, Ovitt TM, Lobkovsky EB, Coates GW. 2001. Polymerization of lactide with zinc and magnesium β-diiminate complexes: Stereocontrol and mechanism. J Am Chem Soc 123:3229–3238.

Cheng J, Khin KT, Davis ME. 2004. Antitumor activity of β-cyclodextrin polymer-camptothecin conjugates. Mol Pharm 1:183–193.

Cheng J, Teply BA, Jeong SY, Yim CH, Ho D, Sherifi I, Jon S, Farokhzad OC, Khademhosseini A, Langer RS. 2006a. Magnetically responsive polymeric microparticles for oral delivery of protein drugs. Pharm Res 23:557–564.

Cheng J, Zeidan R, Mishra S, Liu A, Pun SH, Kulkarni RP, Jensen GS, Bellocq NC, Davis ME. 2006b. Structure—Function correlation of chloroquine and analogues as transgene expression enhancers in nonviral gene delivery. J Med Chem 49:6522–6531.

Cheng J, Teply BA, Sherifi I, Sung J, Luther G, Gu FX, Levy-Nissenbaum E, Radovic-Moreno AF, Langer R, Farokhzad OC. 2007. Formulation of functionalized PLGA-PEG nanoparticles for in vivo targeted drug delivery. Biomaterials 28:869–876.

Chi SL, Pizzo SV. 2006. Angiostatin is directly cytotoxic to tumor cells at low extracellular pH: A mechanism dependent on cell surface-associated ATP synthase. Cancer Res 66:875–882.

Dechy-Cabaret O, Martin-Vaca B, Bourissou D. 2004. Controlled ring-opening polymerization of lactide and glycolide. Chem Rev 104: 6147–6176.

Ellington AD, Szostak JW. 1990. Invitro selection of RNA molecules that bind specific ligands. Nature 346:818–822.

Ellington AD, Szostak JW. 1992. Selection in vitro of single-stranded-DNA molecules that fold into specific ligand-binding structures. Nature 355:850–852.

Esmaeili F, Ghahremani MH, Ostad SN, Atyabi F, Seyedabadi M, Malekshahi MR, Amini M, Dinarvand R. 2008. Folate-receptor-targeted delivery of docetaxel nanoparticles prepared by PLGA-PEG-folate conjugate. J Drug Target 16:415–423.

Farokhzad OC, Jon SY, Khadelmhosseini A, Tran TNT, LaVan DA, Langer R. 2004. Nanopartide-aptamer bioconjugates: A new approach for targeting prostate cancer cells. Cancer Res 64:7668–7672.

Farokhzad OC, Cheng J, Teply BA, Sherifi I, Jon S, Kantoff PW, Richie JP, Langer R. 2006. Targeted nanoparticle-aptamer bioconjugates for cancer chemotherapy in vivo. Proc Natl Acad Sci USA 103:6315–6320.

Gerhardt WW, Noga DE, Hardcastle KI, Garcia AJ, Collard DM, Weck M. 2006. Functional lactide monomers: Methodology and polymerization. Biomacromolecules 7:1735–1742.

Gottschalk C, Frey H. 2006. Hyperbranched polylactide copolymers. Macromolecules 39:1719–1723.

Hagan SA, Coombes AGA, Garnett MC, Dunn SE, Davis MC, Illum L, Davis SS, Harding SE, Purkiss S, Gellert PR. 1996. Polylactide-poly(ethylene glycol) copolymers as drug delivery systems. I. Characterization of water dispersible micelle-forming systems. Langmuir 12:2153–2161.

Hu Y, Jiang XQ, Ding Y, Zhang LY, Yang CZ, Zhang JF, Chen JN, Yang YH. 2003. Preparation and drug release behaviors of nimodipine-loaded poly(caprolactone)-poly(ethylene oxide)-polylactide amphiphilic copolymer nanoparticles. Biomaterials 24:2395–2404.

Huang X, Brazel CS. 2001. On the importance and mechanisms of burst release in matrix-controlled drug delivery systems. J Control Release 73:121–136.

Iijima M, Nagasaki Y, Okada T, Kato M, Kataoka K. 1999. Core-polymerized reactive micelles from heterotelechelic amphiphilic block copolymers. Macromolecules 32:1140–1146.

Ishihara T, Goto M, Kanazawa H, Higaki M, Mizushima Y. 2009. Efficient entrapment of poorly water-soluble pharmaceuticals in hybrid nanoparticles. J Pharm Sci 98:2357–2363.

Jiang M, Wu Y, He Y, Nie J. 2009. Micelles formed by self-assembly of hyperbranched poly (amine-ester)-co-(D,L-lactide) (HPAE-*co*-PLA) copolymers for protein drug delivery. Polym Int 58:31–39.

Jing F, Hillmyer MA. 2008. A bifunctional monomer derived from lactide for toughening polylactide. J Am Chem Soc 130:13826–13827.

Kumar R, Gao W, Gross RA. 2002. Functionalized polylactides: Preparation and characterization of L-lactide-*co*-pentofuranose. Macromolecules 35:6835–6844.

Lai CL, van den Ham R, van Leenders G, van der Lugt J, Mol JA, Teske E. 2008. Histopathological and immunohistochemical characterization of canine prostate cancer. Prostate 68:477–488.

Lee ES, Na K, Bae YH. 2005. Super pH-sensitive multifunctional polymeric micelle. Nano Lett 5:325–329.

Lee SW, Chang DH, Shim MS, Kim BO, Kim SO, Seo MH. 2007. Ionically fixed polymeric nanoparticles as a novel drug carrier. Pharm Res 24:1508–1516.

LeRoy BE, Northrup N. 2009. Prostate cancer in dogs: Comparative and clinical aspects. Vet J 180:149–162.

Liu L, Li CX, Li XC, Yuan Z, An YL, He BL. 2001. Biodegradable polylactide/poly(ethylene glycol)/polylactide triblock copolymer micelles as anticancer drug carriers. J Appl Polym Sci 80:1976–1982.

Lupold SE, Hicke BJ, Lin Y, Coffey DS. 2002. Identification and characterization of nuclease-stabilized RNA molecules that bind human prostate cancer cells via the prostate-specific membrane antigen. Cancer Res 62:4029–4033.

Murdter TE, Friedel G, Backman JT, McClellan M, Schick M, Gerken M, Bosslet K, Fritz P, Toomes H, Kroemer HK, Sperker B. 2002. Dose optimization of a doxorubicin prodrug (HMR 1826) in isolated perfused human lungs: Low tumor pH promotes prodrug activation by β-glucuronidase. J Pharmacol Exp Ther 301:223–228.

Musumeci T, Ventura CA, Giannone I, Ruozi B, Montenegro L, Pignatello R, Puglisi G. 2006. PLA/PLGA nanoparticles for sustained release of docetaxel. Int J Pharm 325:172–179.

Nagasaki Y, Okada T, Scholz C, Iijima M, Kato M, Kataoka K. 1998. The reactive polymeric micelle based on an aldehyde-ended poly (ethylene glycol)/poly(lactide) block copolymer. Macromolecules 31:1473–1479.

Nederberg F, Appel E, Tan JPK, Kim SH, Fukushima K, Sly J, Miller RD, Waymouth RM, Yang YY, Hedrick JL. 2009. Simple approach to stabilized micelles employing miktoarm terpolymers and stereocomplexes with application in paclitaxel delivery. Biomacromolecules 10:1460–1468.

Otsuka H, Nagasaki Y, Kataoka K. 2000. Surface characterization of functionalized polylactide through the coating with heterobifunctional poly(ethylene glycol)/polylactide block copolymers. Biomacromolecules 1:39–48.

Peer D, Karp JM, Hong S, FaroKHzad OC, Margalit R, Langer R. 2007. Nanocarriers as an emerging platform for cancer therapy. Nat Nanotechnol 2:751–760.

Pierri E, Avgoustakis K. 2005. Poly(lactide)-poly(ethylene glycol) micelles as a carrier for griseofulvin. J Biomed Mater Res A 75:639–647.

Soppimath KS, Aminabhavi TM, Kulkarni AR, Rudzinski WE. 2001. Biodegradable polymeric nanoparticles as drug delivery devices. J Control Release 70:1–20.

Southwick PL, Ernst LA, Tauriello EW, Parker SR, Mujumdar RB, Mujumdar SR, Clever HA, Waggoner AS. 1990. Cyanine dye labeling reagents—Carboxymethylindocyanine succinimidyl esters. Cytometry 11:418–430.

Stolnik S, Dunn SE, Garnett MC, Davies MC, Coombes AGA, Taylor DC, Irving MP, Purkiss SC, Tadros TF, Davis SS, Illum L. 1994. Surface modification of poly(lactide-*co*-glycolide) nanospheres by biodegradable poly(lactide)-poly(ethylene glycol) copolymers. Pharm Res 11:1800–1808.

Stolnik S, Heald CR, Neal J, Garnett MC, Davis SS, Illum L, Purkis SC, Barlow RJ, Gellert PR. 2001. Polylactide-poly(ethylene glycol) micellar-like particles as potential drug carriers: Production, colloidal properties and biological performance. J Drug Target 9:361–378.

Sweat SD, Pacelli A, Murphy GP, Bostwick DG. 1998. Prostate-specific membrane antigen expression is greatest in prostate adenocarcinoma and lymph node metastases. Urology 52:637–640.

Teply BA, Tong R, Jeong SY, Luther G, Sherifi I, Yim CH, Khadernhosseini A, Farokhzad OC, Langer RS, Cheng J. 2008. The use of charge-coupled polymeric microparticles and micromagnets for modulating the bioavailability of orally delivered macromolecules. Biomaterials 29:1216–1223.

Tong R, Cheng J. 2008. Paclitaxel-initiated, controlled polymerization of lactide for the formulation of polymeric nanoparticulate delivery vehicles. Angew Chem Int Ed 47:4830–4834.

Tong R, Cheng J. 2010. Controlled synthesis of camptothecin-polylactide conjugates and nanoconjugates. Bioconjugate Chem 21:111–121.

Tong R, Cheng J. 2009. Ring-opening polymerization-mediated controlled formulation of polylactide-drug nanoparticles. J Am Chem Soc 131:4744–4754.

Tong R, Christian DA, Tang L, Cabral H, Baker JR, Kataoka K, Discher DE, Cheng J. 2009. Nanopolymeric therapeutics. MRS Bull 34:422–431.

Tuerk C, Gold L. 1990. Systematic evolution of ligands by exponential enrichment—RNA ligands to bacteriophage-T4 DNA-polymerase. Science 249:505–510.

Verma A, Uzun O, Hu YH, Hu Y, Han HS, Watson N, Chen SL, Irvine DJ, Stellacci F. 2008. Surface-structure-regulated cell-membrane penetration by monolayer-protected nanoparticles. Nat Mater 7:588–595.

Wu Y, Zheng YL, Yang WL, Wang CC, Hu JH, Fu SK. 2005. Synthesis and characterization of a novel amphiphilic chitosan-polylactide graft copolymer. Carbohydr Polym 59:165–171.

Yang L, Wu XH, Liu F, Duan YR, Li SM. 2009. Novel biodegradable polylactide/poly(ethylene glycol) micelles prepared by direct dissolution method for controlled delivery of anticancer drugs. Pharm Res 26:2332–2342.

Zhang L, Gu FX, Chan JM, Wang AZ, Langer RS, Farokhzad OC. 2008. Nanoparticles in medicine: Therapeutic applications and developments. Clin Pharmacol Ther 83:761–769.

Zhang XC, Jackson JK, Burt HM. 1996. Development of amphiphilic diblock copolymers as micellar carriers of taxol. Int J Pharm 132:195–206.

Zhang ZP, Feng SS. 2006a. The drug encapsulation efficiency, in vitro drug release, cellular uptake and cytotoxicity of paclitaxel-loaded poly(lactide)-tocopheryl polyethylene glycol succinate nanoparticles. Biomaterials 27:4025–4033.

Zhang ZP, Feng SS. 2006b. Nanoparticles of poly(lactide)/vitamin E TPGS copolymer for cancer chemotherapy: Synthesis, formulation, characterization and in vitro drug release. Biomaterials 27:262–270.